REPORT NO. FAA-RD-78-115

LEVEL II

1973-1977 ROUGH RIDER TURBULENCE-RADAR INTENSITY STUDY

J.T. Lee
D. Carpenter

March 1979
FINAL REPORT

Prepared for

U.S. DEPARTMENT OF TRANSPORTATION
FEDERAL AVIATION ADMINISTRATION
Systems Research & Development Service
Washington, D.C. 20590

NOTICE

This document is disseminated under the sponsorship of the Department of Transportation in the interest of information exchange. The United States Government assumes no liability for its contents or use thereof.

Technical Report Documentation Page

1. Report No.	2. Government Accession No.	3. Recipient's Catalog No.
FAA-RD-78-115		

4. Title and Subtitle	5. Report Date
1973-1977 Rough Rider Turbulence-Radar Intensity Study.	March 1979
	6. Performing Organization Code
7. Author(s) J. T. Lee, D. M. Carpenter	8. Performing Organization Report No. 38p.
9. Performing Organization Name and Address U.S. Dept. of Commerce National Oceanic and Atmospheric Administration National Severe Storms Laboratory 1313 Halley Circle, Norman, Oklahoma 73069	10. Work Unit No. (TRAIS) 244670 11. Contract or Grant No. DOT-FA77WAI-808
12. Sponsoring Agency Name and Address U.S. Department of Transportation Federal Aviation Administration Systems Research and Development Service Washington, D.C. 20590	13. Type of Report and Period Covered Final Report, April 1977 - June 1978 14. Sponsoring Agency Code FAA/ARD-450

15. Supplementary Notes

Prepared under FAA Interagency Agreement No. DOT-FA77WAI-808, managed by the Aviation Weather Branch, ARD-450

16. Abstract

Thunderstorm turbulence is a weather hazard to safe aircraft flight. A joint program by the Federal Aviation Administration, the U.S. Air Force's Aeronautical Systems Command, and the National Oceanic and Atmospheric Administration's National Severe Storms Laboratory was renewed in 1973. Used in conjunction with ground based standard weather radar and Doppler weather radar was a F-4-C aircraft instrumented to research turbulence, wind, and temperature during thunderstorm penetrations. Results of these flights are presented and compared with studies made 10 or more years previous. These show that as the intensity of a storm increases, the probability of encountering moderate or greater turbulence somewhere in the storm also increases. Encounters of moderate turbulence are nearly ten times more frequent when the storm's maximum reflectivity is 60 dBZ or greater than when it is 40 to 49 dBZ. There is little correlation between turbulence intensity and distance from the aircraft to center of storm at the time when the turbulence was recorded.

17. Key Words	18. Distribution Statement
Thunderstorm Radar Turbulence	Document is available to the U.S. public through the National Technical Information Service, Springfield, Virginia 22151

19. Security Classif. (of this report)	20. Security Classif. (of this page)	21. No. of Pages	22. Price
Unclassified	Unclassified	27	

Form DOT F 1700.7 (8-72) Reproduction of completed page authorized

S/N 244670

PREFACE

The authors are grateful to all who helped in the preparation of this report. In particular, we would like to thank the pilots [Major Douglas Cairns (1973), Capt. Frederick Gregory (1974), Major Clarence Bogemann (1975), Lt. Cmdr. Steven Hastings (1976) and Capt. James Dunn (1977)]. Mr. Larry Roberts was Flight Test Engineer for the program, except in 1975 when Mr. Drake Daum flew in his place, and there were other Aeronautical System Division crew and staff that made the flights possible. We also want to express our appreciation to the FAA Air Traffic Controllers working with us. Mr. Jess Jennings', Mr. Glen Anderson's and Mr. Dale Sirmans' support in the radar maintenance and engineering were essential ingredients in the project's success as were the efforts of many other NSSL staff members. We also express our thanks to Mrs. Evelyn Horwitz, who did the secretarial work for this report.

METRIC CONVERSION FACTORS

Approximate Conversions to Metric Measures

Symbol	When You Know	Multiply by	To Find	Symbol
		LENGTH		
in	inches	*2.5	centimeters	cm
ft	feet	30	centimeters	cm
yd	yards	0.9	meters	m
mi	miles	1.6	kilometers	km
		AREA		
in^2	square inches	6.5	square centimeters	cm^2
ft^2	square feet	0.09	square meters	m^2
yd^2	square yards	0.8	square meters	m^2
mi^2	square miles	2.6	square kilometers	km^2
	acres	0.4	hectares	ha
		MASS (weight)		
oz	ounces	28	grams	g
lb	pounds	0.45	kilograms	kg
	short tons (2000 lb)	0.9	tonnes	t
		VOLUME		
tsp	teaspoons	5	milliliters	ml
Tbsp	tablespoons	15	milliliters	ml
fl oz	fluid ounces	30	milliliters	ml
c	cups	0.24	liters	l
pt	pints	0.47	liters	l
qt	quarts	0.95	liters	l
gal	gallons	3.8	liters	l
ft^3	cubic feet	0.03	cubic meters	m^3
yd^3	cubic yards	0.76	cubic meters	m^3
		TEMPERATURE (exact)		
°F	Fahrenheit temperature	5/9 (after subtracting 32)	Celsius temperature	°C

*1 in = 2.54 (exactly). For other exact conversions and more detailed tables, see NBS Misc. Publ. 286, Units of Weights and Measures, Price $2.25, SD Catalog No. C13.10:286.

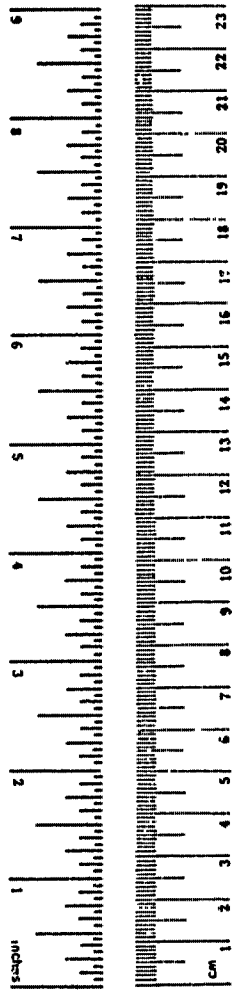

Approximate Conversions from Metric Measures

Symbol	When You Know	Multiply by	To Find	Symbol
		LENGTH		
mm	millimeters	0.04	inches	in
cm	centimeters	0.4	inches	in
m	meters	3.3	feet	ft
m	meters	1.1	yards	yd
km	kilometers	0.6	miles	mi
		AREA		
cm^2	square centimeters	0.16	square inches	in^2
m^2	square meters	1.2	square yards	yd^2
km^2	square kilometers	0.4	square miles	mi^2
ha	hectares (10,000 m^2)	2.5	acres	
		MASS (weight)		
g	grams	0.035	ounces	oz
kg	kilograms	2.2	pounds	lb
t	tonnes (1000 kg)	1.1	short tons	
		VOLUME		
ml	milliliters	0.03	fluid ounces	fl oz
l	liters	2.1	pints	pt
l	liters	1.06	quarts	qt
l	liters	0.26	gallons	gal
m^3	cubic meters	35	cubic feet	ft^3
m^3	cubic meters	1.3	cubic yards	yd^3
		TEMPERATURE (exact)		
°C	Celsius temperature	9/5 (then add 32)	Fahrenheit temperature	°F

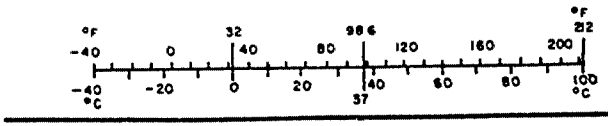

TABLE OF CONTENTS

LIST OF ILLUSTRATIONS

LIST OF ILLUSTRATIONS (cont.)

LIST OF ILLUSTRATIONS (cont.)

LIST OF ILLUSTRATIONS (cont.)

LIST OF TABLES

LIST OF ABBREVIATIONS AND SYMBOLS

C	=	Constant
C_{L_α}	=	Aircraft lift curve slope
CST	=	Central Standard Time
dBZ	=	Radar reflectivity factor in decibels
ft	=	feet
fps	=	feet per second
K	=	dielectric factor
K_g	=	gust alleviation factor
km	=	Kilometers
m	=	meter
$m\ s^{-1}$	=	meter per second
n mi	=	nautical mile
P_r	=	power received
P_t	=	power transmitted
r	=	range
S	=	wing area
s	=	second
U_{de}	=	derived gust velocity
V_e	=	equivalent air speed at sea level
W	=	weight of aircraft
Z_e	=	radar reflectivity
ρ_o	=	air density at sea level

1973-1977 ROUGH RIDER TURBULENCE-RADAR INTENSITY STUDY

1.0 INTRODUCTION

1.1 Purpose

The program objective is to determine to what extent radar reflectivity correlates with turbulent areas measured by aircraft.

1.2 Background

In 1973 a joint experiment was begun by the Federal Aviation Administration (FAA), Air Force (AF) and the National Oceanic and Atmospheric Administration's (NOAA) National Severe Storms Laboratory (NSSL). This joint effort centered on in-situ measurements of turbulent regions by penetration aircraft (Figures 1 and 2) and simultaneous probing by NSSL's 10 cm Doppler radar (Figure 3) and the WSR-57 weather radar (Figure 4). During this program, turbulence data were acquired by the aircraft while concurrent measurements were made of radial wind speed, velocity spectrum width and radar reflectivity intensity using Doppler and weather radars. This report addresses the aircraft measured turbulence and radar reflectivity observations.

1.2.1 Program Operations

An F-100 aircraft from the 4950th Test Wing, Wright-Patterson Air Force Base, Air Force Systems Command (AFSC) was used in 1973 and 1974. In 1975, the F-100 was replaced by an F-4-C. The 4950th Test Wing flew the aircraft until 1976 when it was transferred to the 3246 Test Wing AFSC at Eglin AFB and operated by them in 1976 and 1977. Mr. Larry Roberts, of the 4950th, was the aircraft instrumentation and data processing supervisor during these flights. Tinker Air Force Base (TIK), 20 km (11 n. mi.) northeast of NSSL, was used as the program's aircraft operation base.

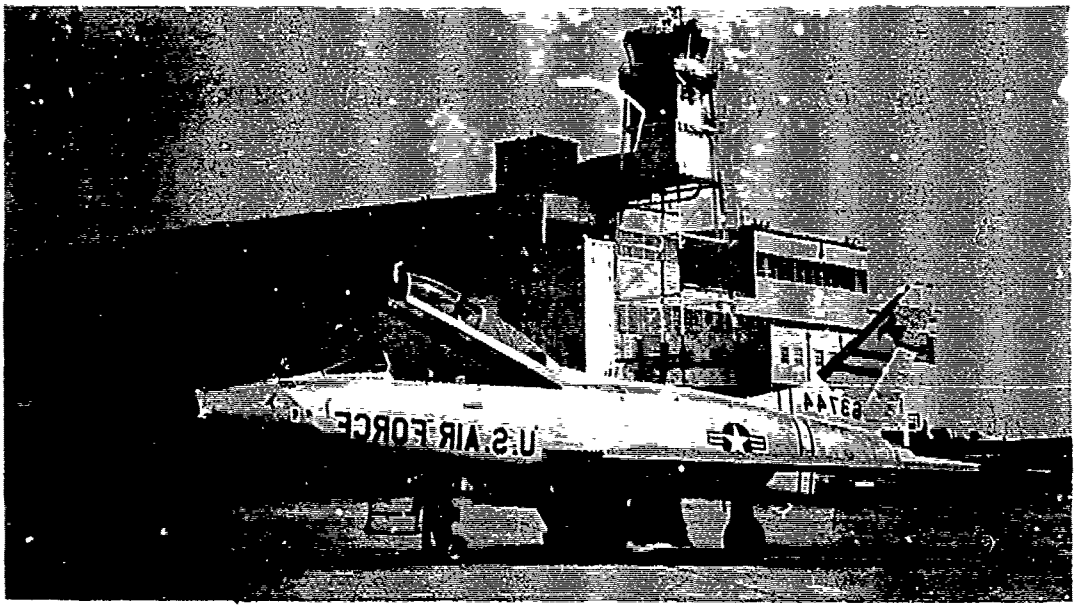

Figure 1. Air Force Systems Command's F-100 aircraft used in thunderstorm turbulence investigations (1973-1974).

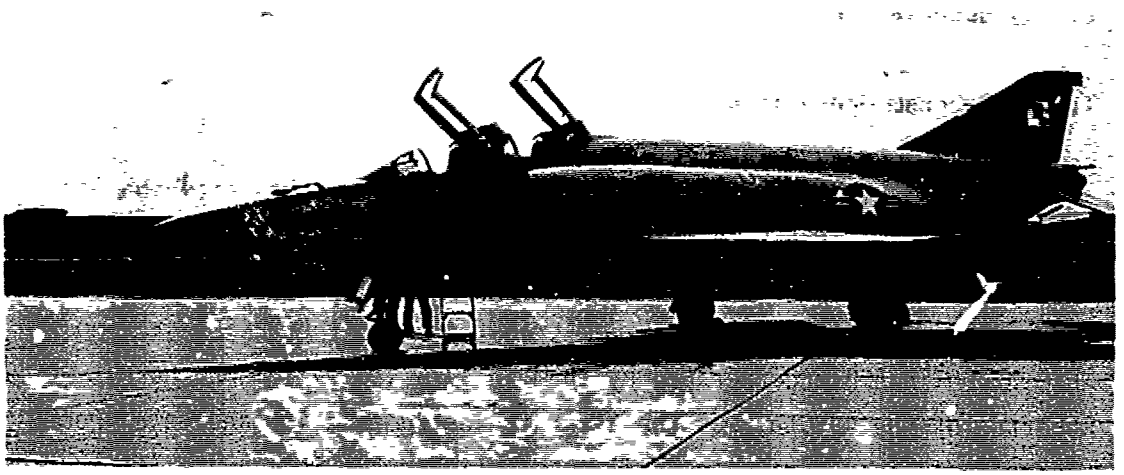

Figure 2. Air Force Systems Command's F-4-C aircraft used in test program (1975-1977).

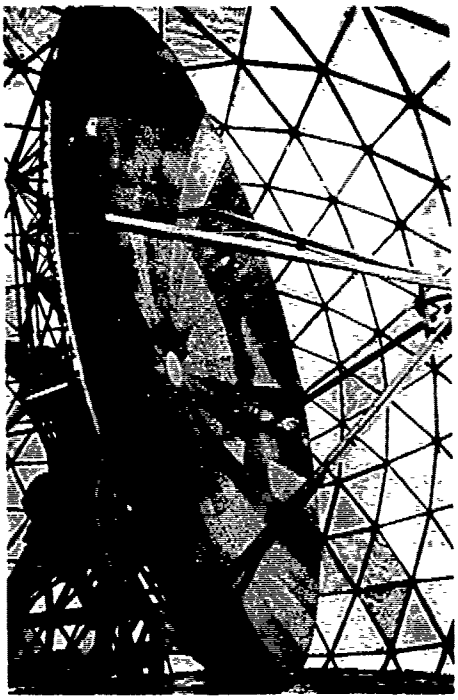

Figure 3. 30 ft. diameter Doppler radar antenna at NSSL.

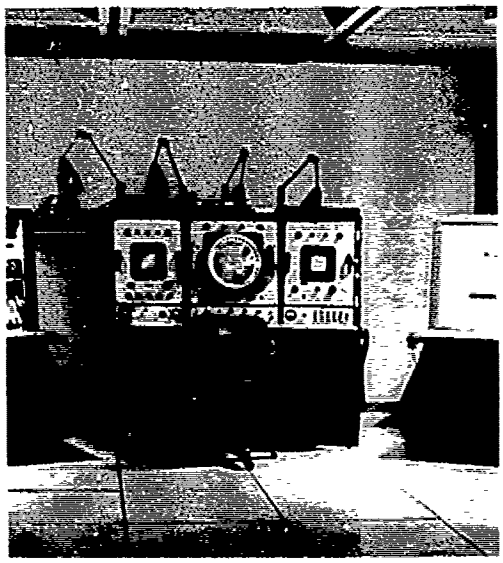

Figure 4. WSR-57 radar console at NSSL.

During penetrations, the aircraft is under the direct control of an FAA air traffic controller collocated at NSSL's weather and Doppler radar display. Transponder (IFF) information is electronically superimposed on the Plan Position Indicator (PPI) radar scope to locate and track the aircraft (figure 5). Turbulence data consisting of normal acceleration at the center of gravity, boom vane angles, angle of attack, pitch rate, airspeed, altitude and other required data are recorded on magnetic tape in the aircraft. Conversion to meteorological engineering units is accomplished during computer data processing. Data are sampled at 50 per sec and a five point smoothed average provides 0.1 sec values used

in computations. In this report, we limit discussion to a measure of turbulence called derived gust velocity (U_{de}) (Pratt and Walker, 1954)

where

$$U_{de} = \frac{2\,\Delta_n\, W}{V_e K_g \rho_o C_{L_\alpha} S}$$

With

Δ_n = incremental vertical acceleration of aircraft (from normal)

W = weight of aircraft

V_e = equivalent air speed at sea level

ρ_o = air density at sea level

C_{L_α} = aircraft lift curve slope

K_g = gust alleviation factor

S = wing area

Radar data are recorded on magnetic tape in digital format and also on film. Data are recorded at 0° elevation angles before and after each penetration. During penetrations the Doppler and weather radar antennas are programmed through a tilt sequence encompassing the penetration altitude. Time signals from WWV are used to synchronize the radar and aircraft data.

Figure 5. WSR-57 weather radar reflectivity iso-echo contour display with aircraft transponder beacons superimposed. Point A is the beacon return from the F-100. The dotted line indicates the aircraft track. Contour levels are approximately 10, 20, 30 (second block), 40 and 50 dBZ. Range marks are at 40 km intervals.

Radar reflectivities (Z_e) of storm areas are obtained from the following simplified radar equation (Burnham and Lee, 1969):

$$Z_e \text{ (dBZ)} = 10 \log Z_e$$

$$Z_e = \overline{P}_r \, r^2 / P_t \, C \, |K|^2$$

$\overline{P}_r$ = mean power received

P_t = power transmitted

r = range

C = a constant applicable to each particular radar system

K = dielectric factor of the target

1.2.2 Programed Analysis

The first study in the series addressed is the radar reflectivity-turbulence correlation for storms with maximum radar reflectivity levels = 30, 40, 50, 60, and 70 dBZ. The data set contained no storms having Z_e greater than or equal to 70 dBZ. The second study is the correlation of turbulence as a function of the distances from the flight path to the centroid of reflectivity and to the nearest point for specific reflectivity levels.

Results, along with some explanation of the methods used, are discussed below.

2.0 Data

Shown in Table 1 are the number of penetrations included for storms having a given maximum reflectivity, and the total flights included from each year. Penetrations of storms with a maximum reflectivity between 40 and 49 dBZ are the most numerous, and constitute the most reliable data

Table 1. Number of Rough Rider Thunderstorm Penetrations 1973-1977.

Year	Number of Penetrations 30-39 dBZ	Number of Penetrations 40-49 dBZ	Number of Penetrations 50-59 dBZ	Number of Penetrations 60-69 dBZ	Total
1973	1	16	9	1	27
1974	5	13	14	0	43
1975	3	8	15	0	26
1976	2	14	2	0	18
1977	3	36	0	0	39
Totals	14	98	40	1	153

set. Only one penetration of a storm with a maximum reflectivity between 60 and 69 dBZ was accomplished and any inference from the analysis is questionable. The remaining three categories of penetrations provide a reasonable assessment of the actual distribution of gust velocity intensity with respect to reflectivity values within a storm and with respect to the aircraft's distance from those values.

One consideration should be taken into account when studying these data; the flight paths are not necessarily similar from one storm to another. Since the data were originally collected to satisfy a different project objective, various altitudes and flight tracks were flown. Thus, it is possible that the data are biased, especially in the higher reflectivity storms, where penetrations were made through expected zones of light turbulence.

3. Correlation with Maximum Reflectivity of the Storm

The results of the first task are illustrated by Figures 6a, 6b, 7a and 7b. These four figures represent the mean number of occurrences of the abscissa value gust velocities per 10 km and 10 n. mi. of flight, respectively, encountered in storms with specific maximum reflectivities.

Figures 6a and 6b show the mean number of occurrences before smoothing. These values are arithmetic averages of recorded gust occurrences. Each symbol represents a range (10 dBZ) of Z_{max}, and is positioned such that the symbol's center indicates the point to be graphed. Note that encounters of light turbulence are much more frequent than moderate or severe turbulence encounters. The distribution is approximately exponential, and does not seem to deviate greatly from expectations. The only outstanding feature shows up in the distribution of points corresponding to Z_{max} between 60 and 69 dBZ. It is assumed that these values would have a distribution closer to exponential had there been more penetrations in storms with this maximum reflectivity. These figures also show that as the reflectivity of a storm increases, the probability of turbulence inc

Figures 7a and 7b more clearly illustrate this observation and are smoothed versions of figures 6a and 6b with the ordinate axis now being the log of the number of occurrences of the abscissa value. A least squares line was fitted to the log of the original values. All lines except the one corresponding to Z_{max} from 50 to 59 dBZ, have similar slopes. The bias in this one line may be due to the difference in the flight path selected for storms with reflectivities greater than 50 dBZ. In order to avoid hail damage to the aircraft, areas with reflectivity of 50 dBZ or greater were avoided. Thus, the higher magnitude gust velocities which one might associate with areas closer to the updraft of a storm were probably avoided. The line for Z_{max} greater than 60 dBZ is noticeably short due to the lack of data. Correlation coefficients and standard errors of lines are shown in Table 2.

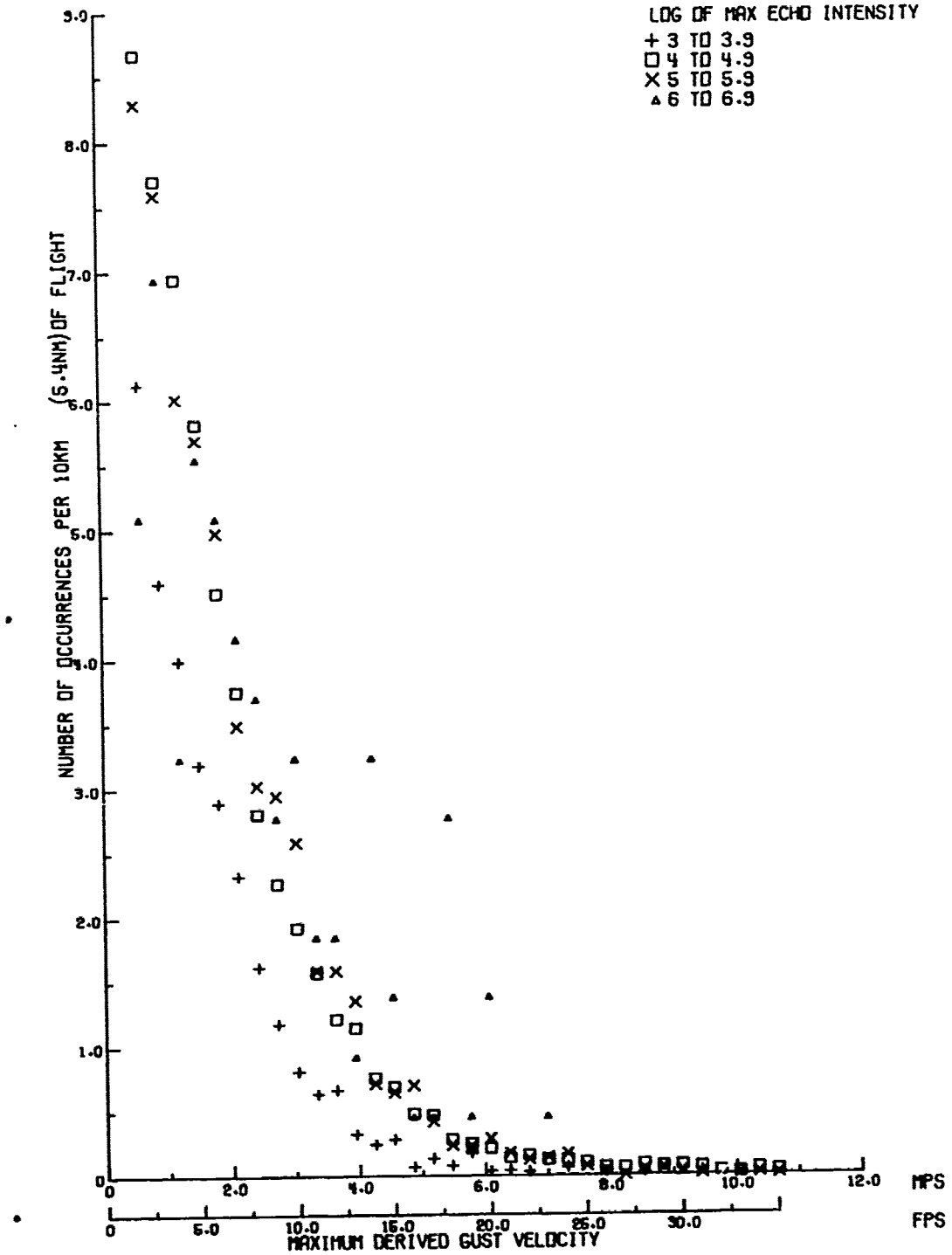

Figure 6a. Mean frequency of derived gust velocity occurrences encountered during penetrations through storms. Categorized maximum radar reflectivity; mean frequencies are normalized to 10 km of thunderstorm flight.

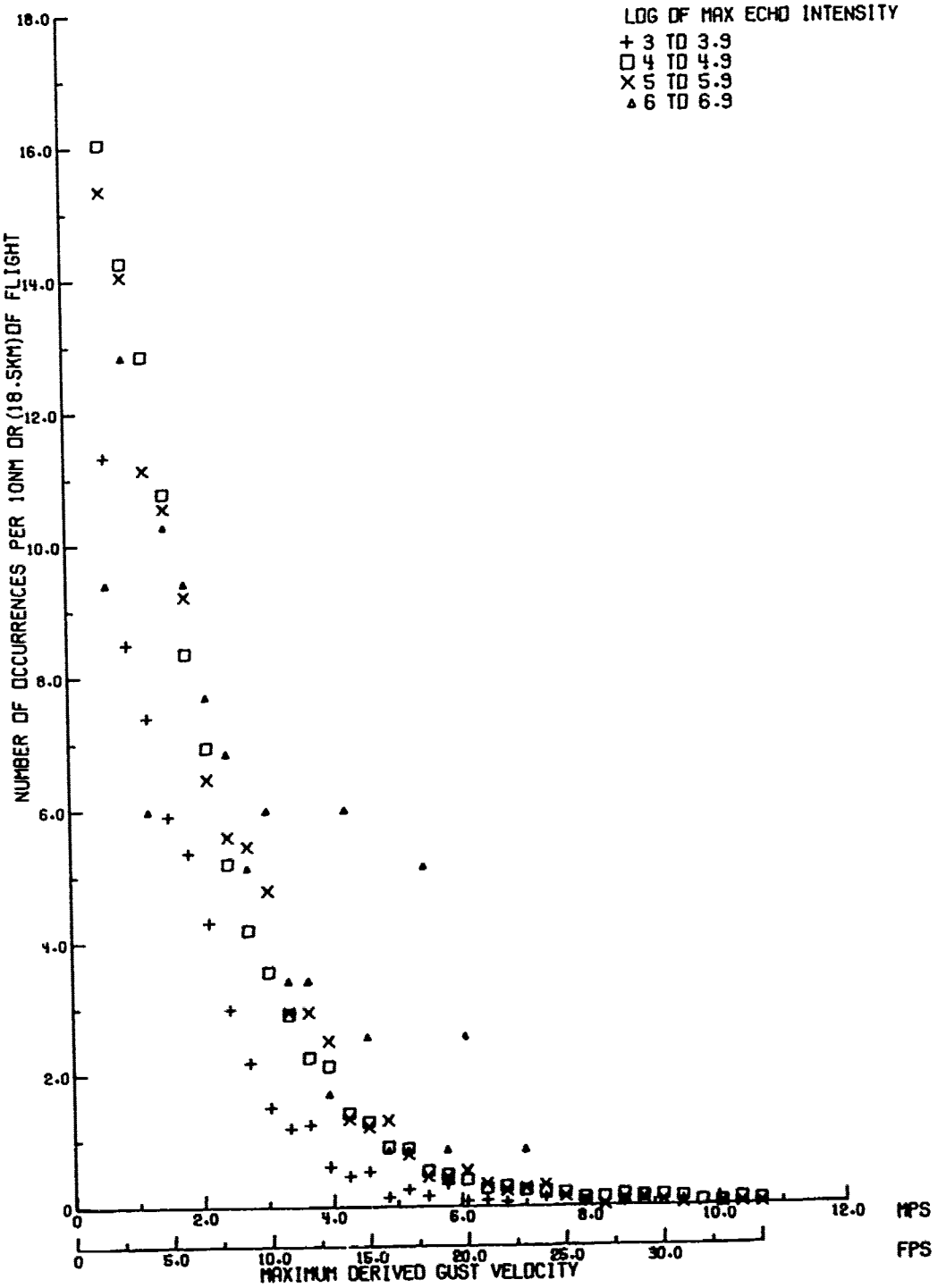

Figure 6b. Same as Figure 6a except that the number of occurrences are for 10 n mi of thunderstorm flight.

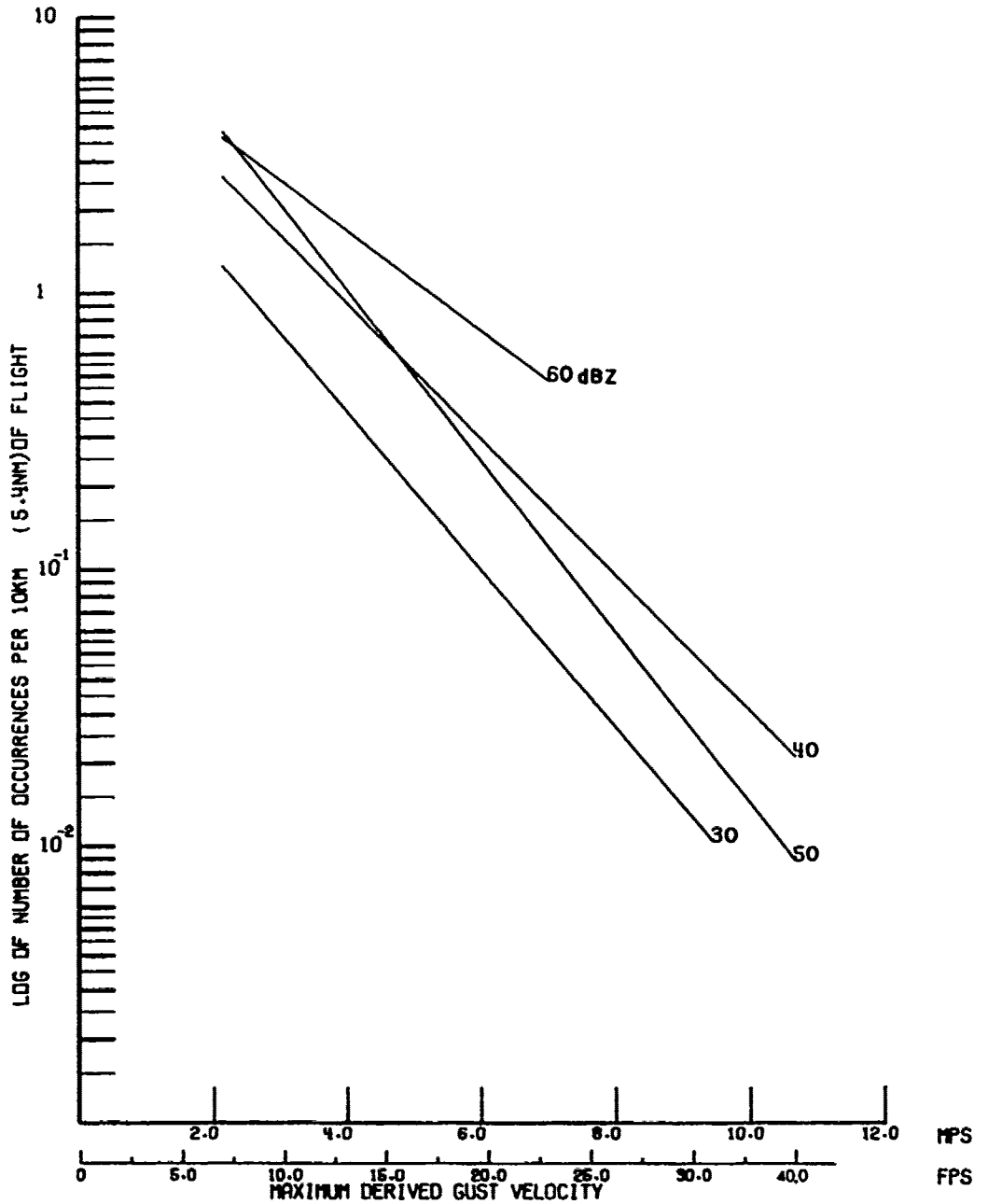

Figure 7a. Smoothed frequency of derived gust velocity occurrence encountered during penetrations through storms. Categorized maximum radar reflectivity; frequency of occurrences normalized to 10 km of thunderstorm flight.

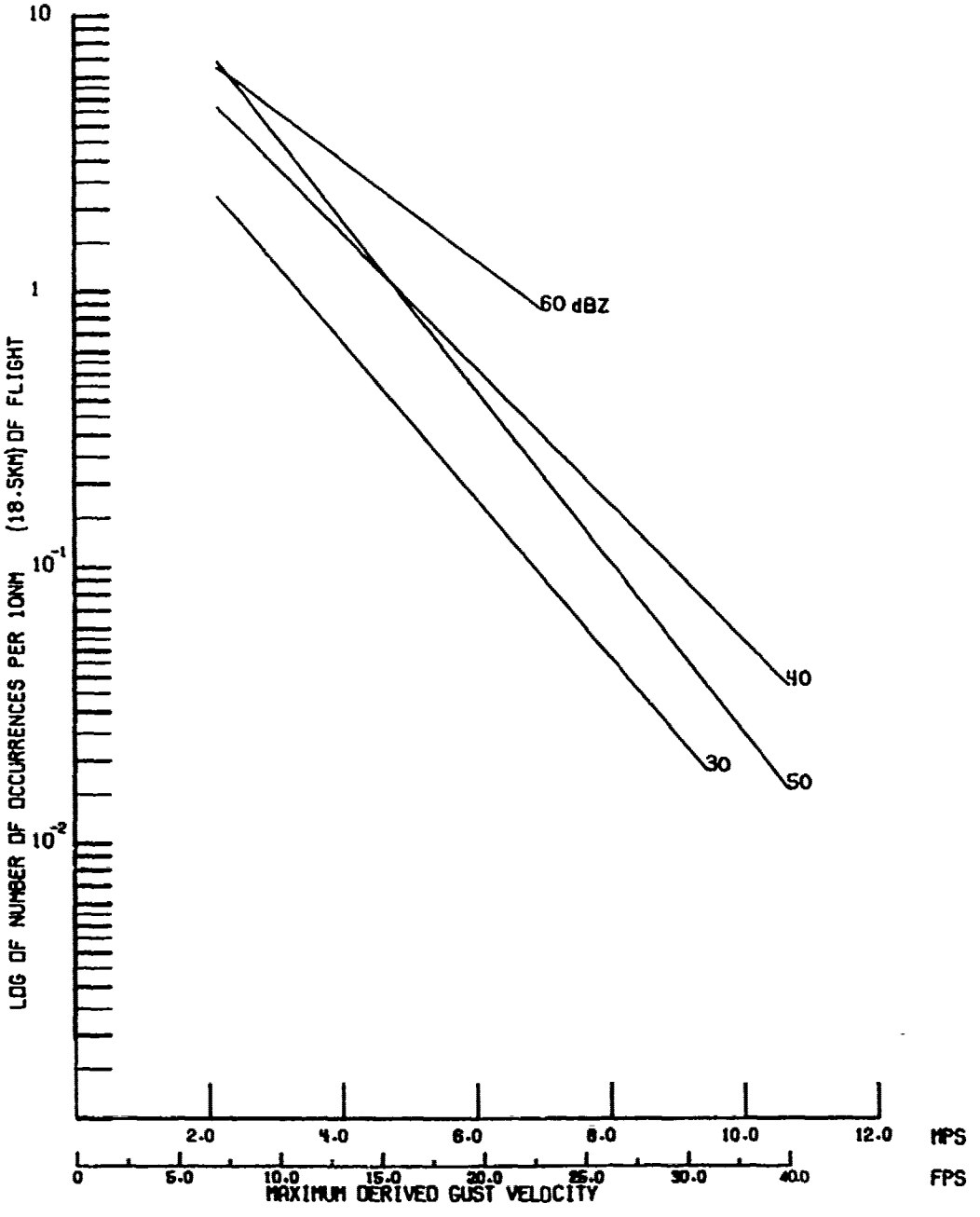

Figure 7b. Same as Figure 7a except occurrences are per 10 n mi of flight.

Table 2. Frequency of Occurred Regression Equations

Regression Equation When Maximum Reflectivity of Storm is:	Standard Error	Correlation Coefficient
30 dBZ	0.255	-0.912
40 dBZ	0.139	-0.978
50 dBZ	0.226	-0.964

A look at these figures reveals that all lines represent their distribution with acceptable accuracy. This is even true for the 60 dBZ or greater line, since the sample size is dependent on the number of gusts recorded rather than the number of penetrations.

In Figure 8 is a comparison of Figure 7b with results of penetrations made during 1964-1965 by F-100 (84 penetrations), F-11 (40 penetrations) and a British Scimitar (54 penetrations) aircraft reported by Lee (1965) and Burnham and Lee (1969). Note the somewhat higher frequency of turbulence occurrence during these earlier flights, which were predominantly made above 6 km (20,000 ft). These flights also were directed through suspected severe turbulence zones and thus the frequency of turbulence occurrences per flight distance in thunderstorm may well be higher.

4.0 Correlation with Distance to Centroid

Figures 9 through 12 indicate the range, mean, and percentage of total gusts above six meters per second (moderate turbulence or more) vis-a-vis the distance to the storm's centroid. Gust velocities are on the ordinate, the distance to the centroid is on the abscissa. The top axis depicts the percentage of the total number of gusts recorded in storms of the given values of maximum reflectivity (e.g., 30 dBZ = 30 - 39 dBZ).

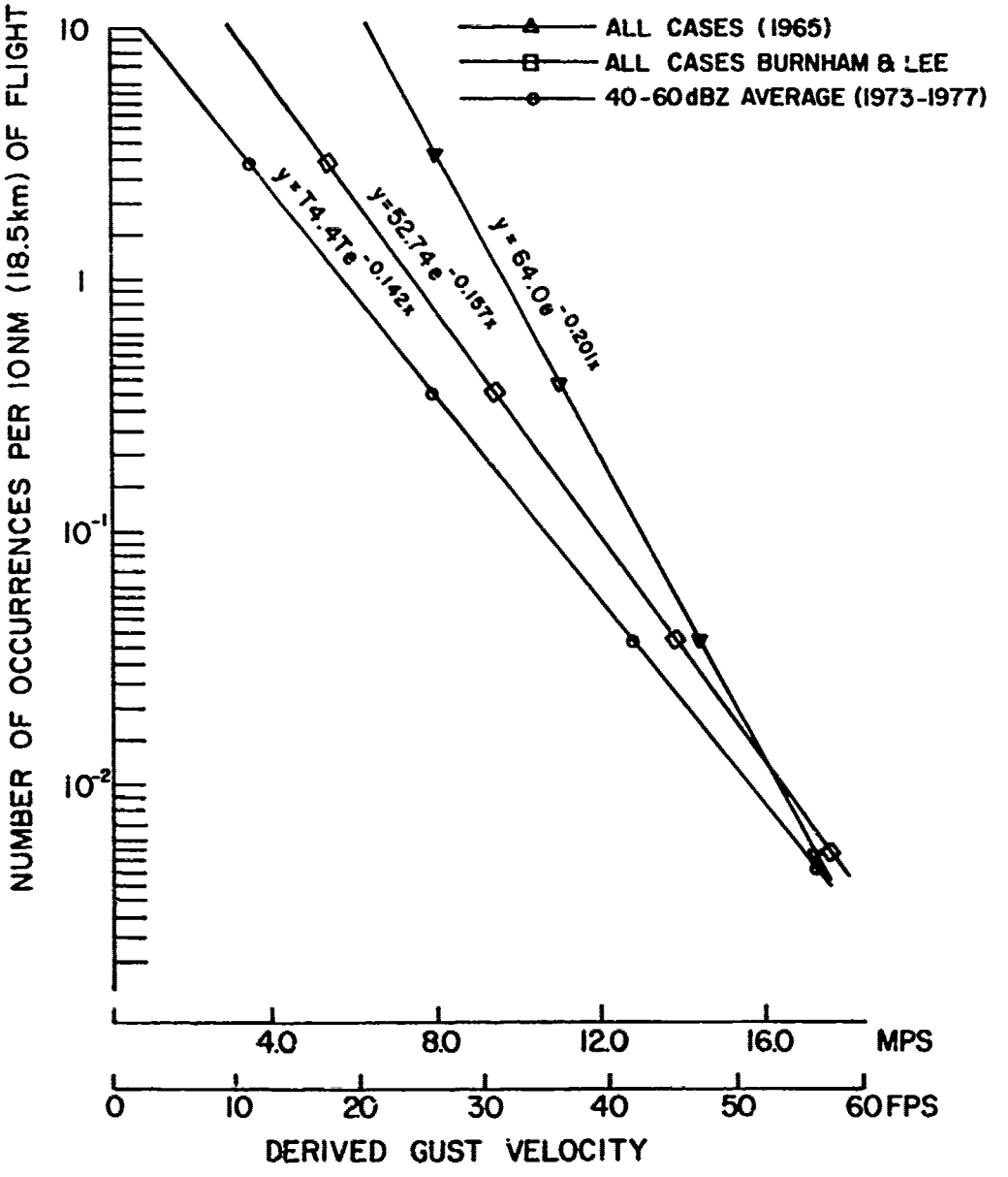

Figure 8. Frequency of turbulence encounters observed 1973-1977, as compared to observations made during the mid-1960's. Equations are exponential corresponding to the least square best fit for the data shown.

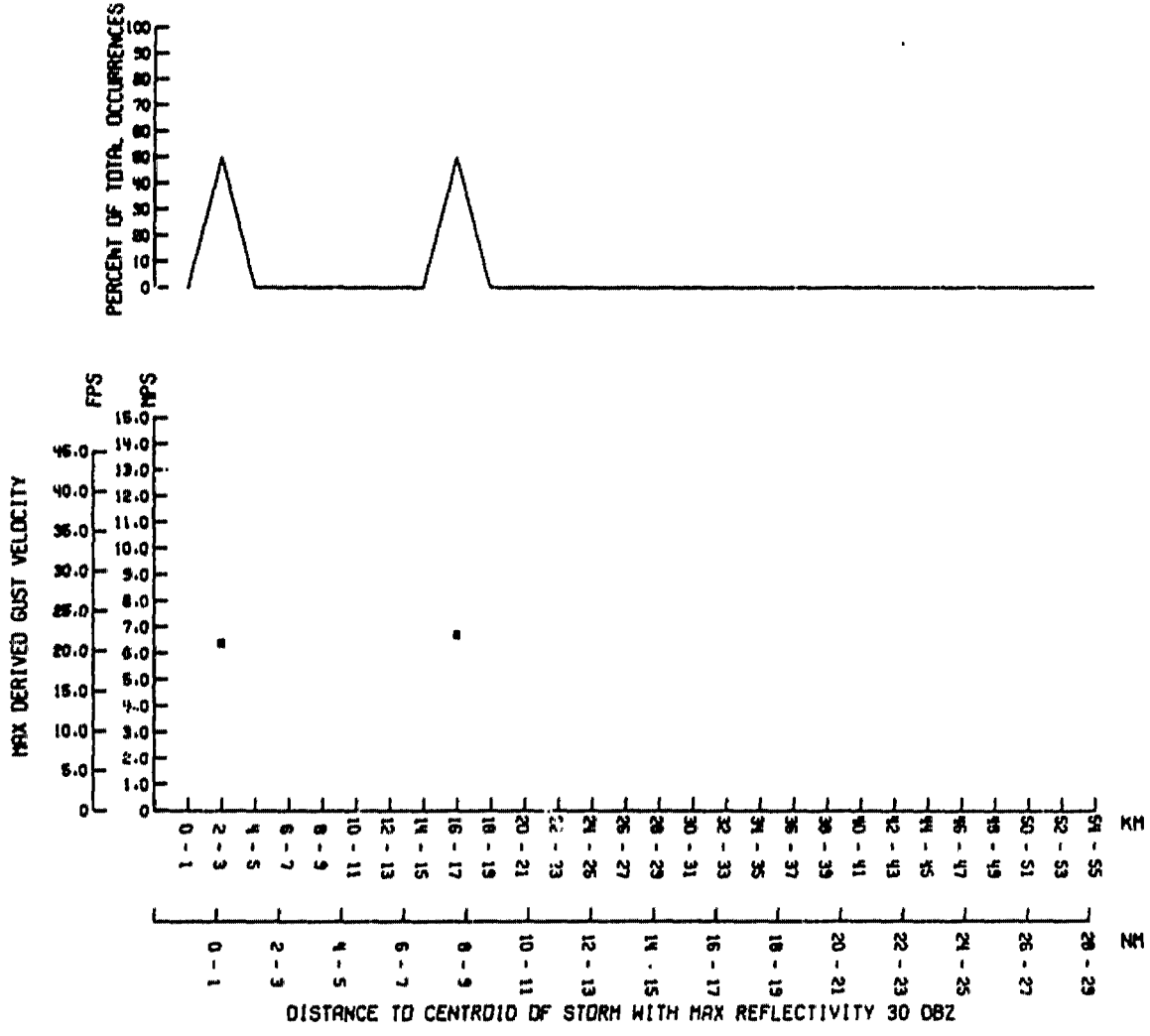

Figure 9. Distribution of derived gust velocity occurrences exceeding 6 m s^{-1} with respect to distance from point of encounter to center of storm --30 to 39 dBZ storms.

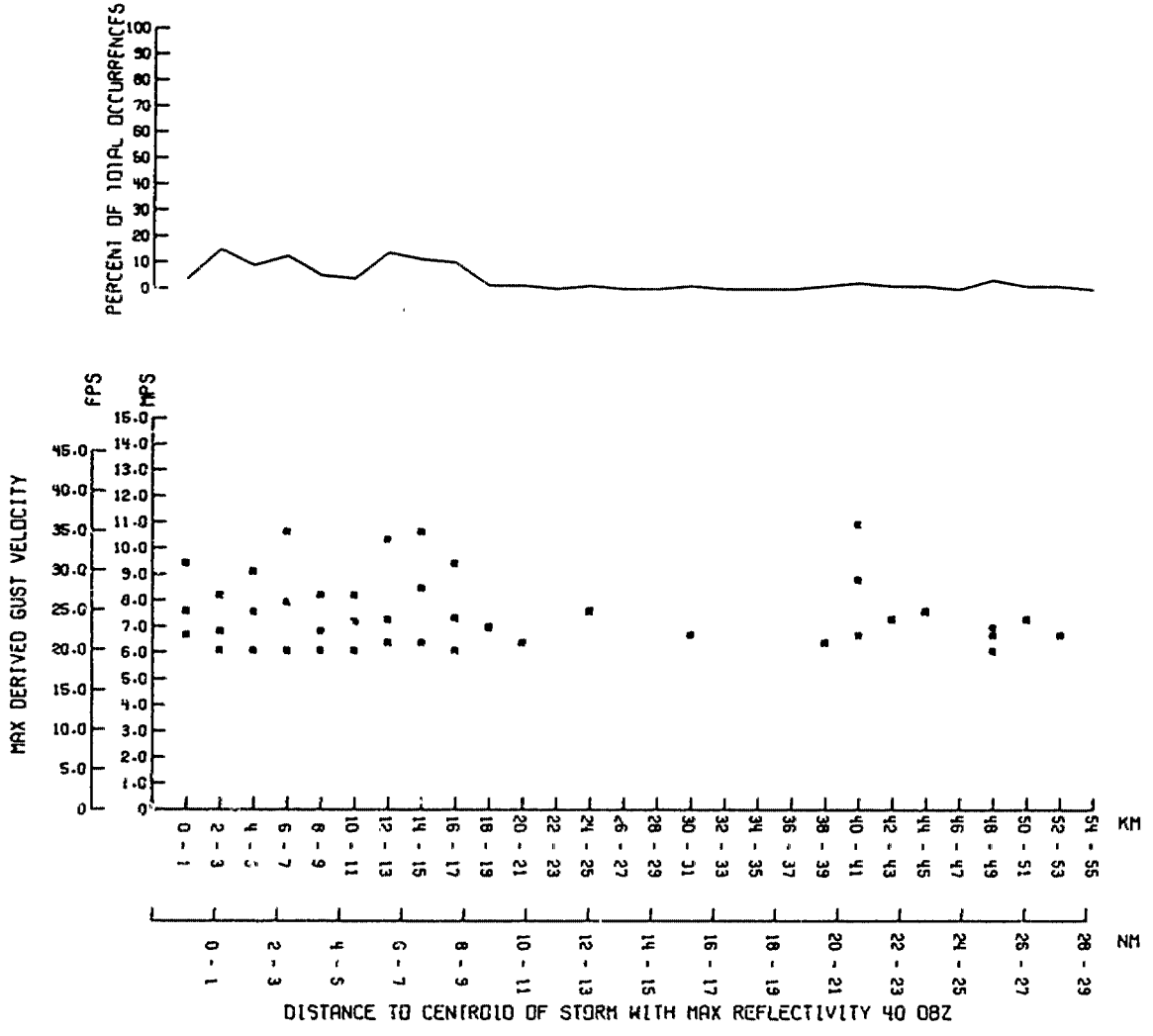

Figure 10. Distribution of derived gust velocity occurrences exceeding 6 m s^{-1} with respect to distance from point of encounter to center of storm --40 to 49 dBZ storms.

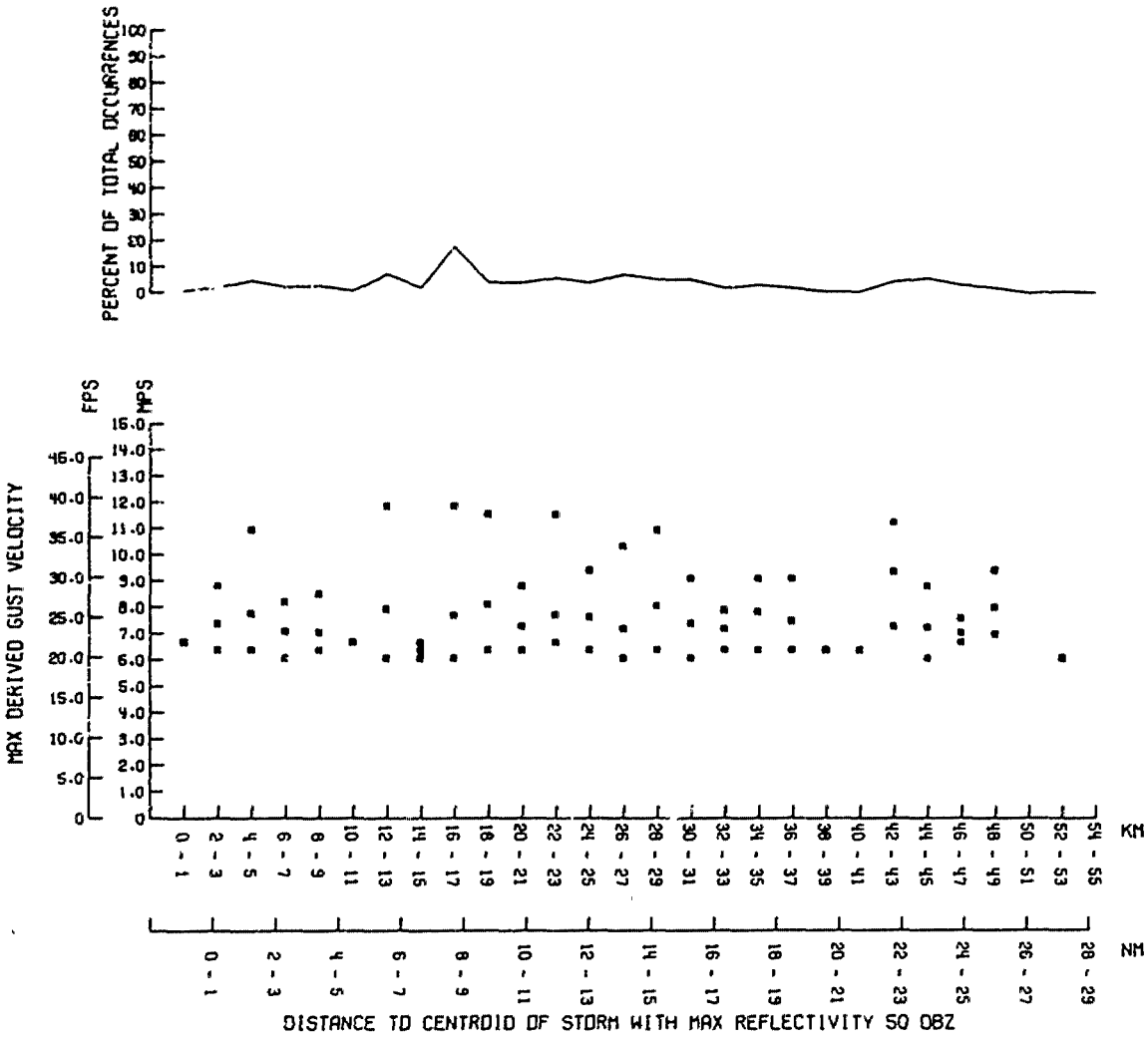

Figure 11. Distribution of derived gust velocity occurrences exceeding 6 m s^{-1} with respect to distance from point of encounter to center of storm --50 to 59 dBZ storms.

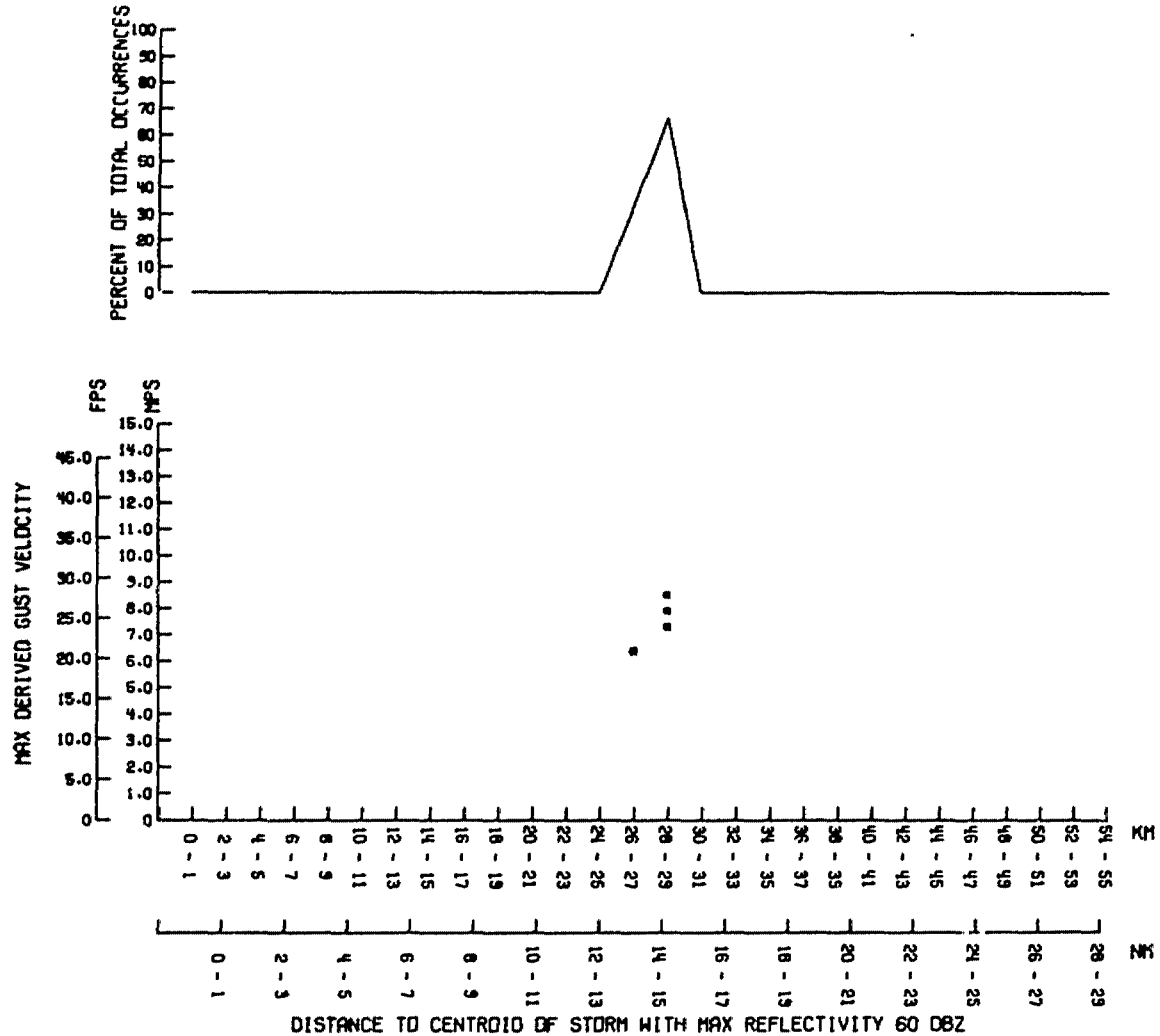

Figure 12. Distribution of derived gust velocity occurrence exceeding 6 m s^{-1} with respect to distance from point of encounter to center of storm --60 dBZ or greater storms.

Derived gust velocity maximum, mean, and minimum values are located by asterisks plotted relative to increments of distance to the centroid of the storm. If these three points should happen to coincide, only one point is plotted.

Figures 10 and 11 give the best indication of the distribution of gust velocity with respect to the centroid of the storm. One might expect that a greater percentage of gusts would be encountered nearer the centroid in Figure 11 if the flight paths in these storms had actually been closer to the centroid.

Figure 9 illustrates the infrequency of gusts with magnitudes greater than 6 mps in storms with a Z_{max} less than 40 dBZ. Figure 12 is of little significance due to the lack of data.

5.0 Correlation with Reflectivity Levels

Figures 13 through 22 illustrate the distribution of gusts with respect to the distance from a particular value of reflectivity for each of the four storm categories. All figures show that there is essentially no correlation between the distance to a certain value of reflectivity and the magnitude of the gust experienced.

6.0 Penetration Maximum Gust and Storm Intensity

Correlations were computed between the largest value of derived gust velocity experienced in a penetration and the storm's maximum value, and between the gust and the maximum value of reflectivity along the flight path (Table 3).

As expected, the correlation is again very poor and is biased by the numerous cases when only light turbulence was experienced during penetration. This location of light turbulence areas is an objective germane to the primary data sampling procedure stated in the introduction. Therefore, while the flight program adequately fulfilled the original purpose, it does not satisfy the objective observing maximum possible turbulence.

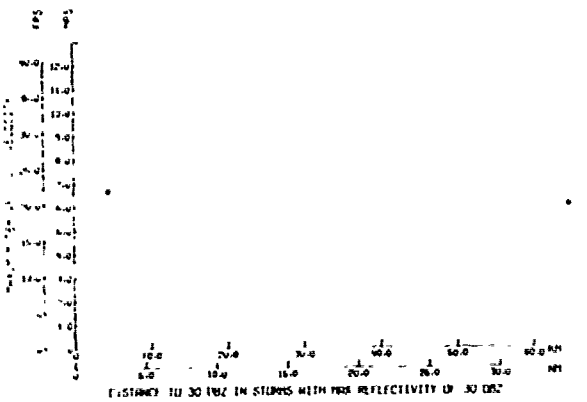

Figure 13. Distribution of derived gust velocity occurrences exceeding 6 m s^{-1} with respect to distance between occurrence and nearest 30 dBZ reflectivity contour when storm's maximum reflectivity is 30-39 dBZ.

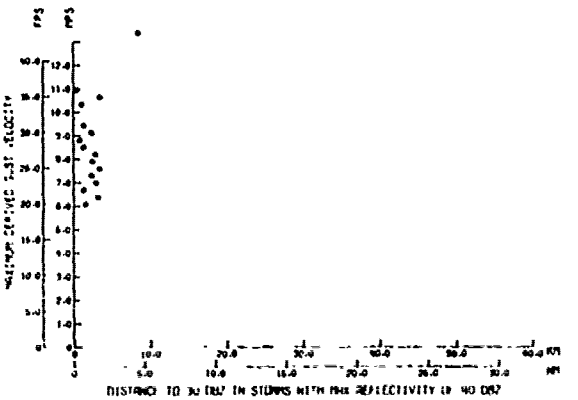

Figure 14. Distribution of derived gust velocity occurrences exceeding 6 m s^{-1} with respect to distance from 30 dBZ contour when maximum reflectivity is 40-49 dBZ.

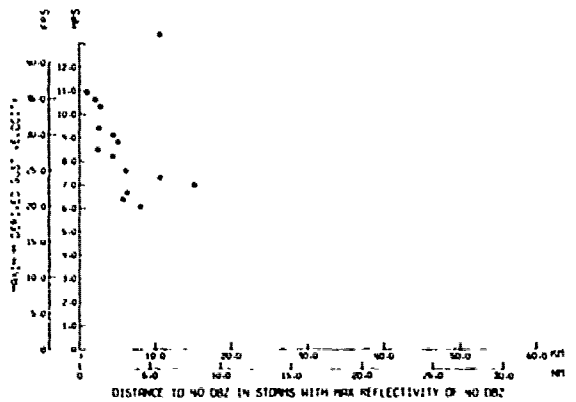

Figure 15. Distribution of derived gust velocity occurrences exceeding 6 m s^{-1} with respect to distance from 40 dBZ contour when maximum reflectivity is 40-49 dBZ.

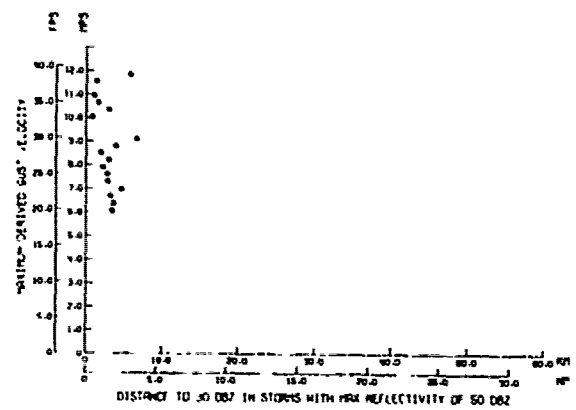

Figure 16. Distribution of derived gust velocity occurrences exceeding 6 m s^{-1} with respect to distance between occurrence and nearest 30 dBZ contour when storm's maximum reflectivity is 50 to 59 dBZ.

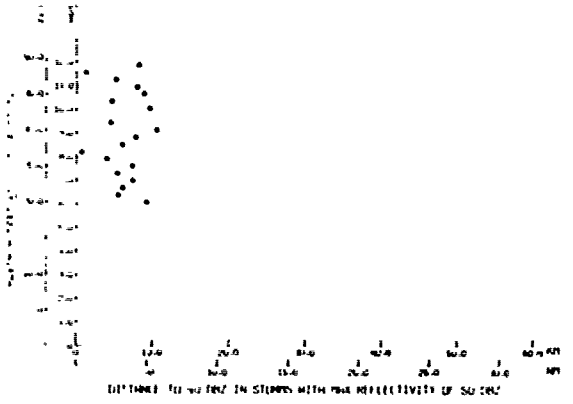

Figure 17. Distribution of derived gust velocity occurrences exceeding 6 m s^{-1} with respect to distance between occurrence and nearest 40 dBZ contour when storm's maximum reflectivity is 50 to 59 dBZ.

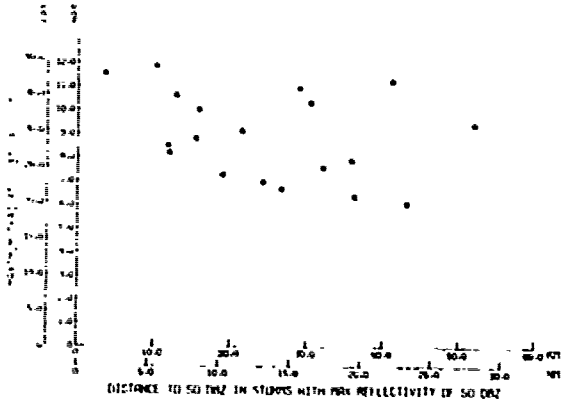

Figure 18. Distribution of derived gust velocity occurrences exceeding 6 m s^{-1} with respect to distance between occurrence and nearest 50 dBZ contour when storm's maximum reflectivity is 50 to 59 dBZ.

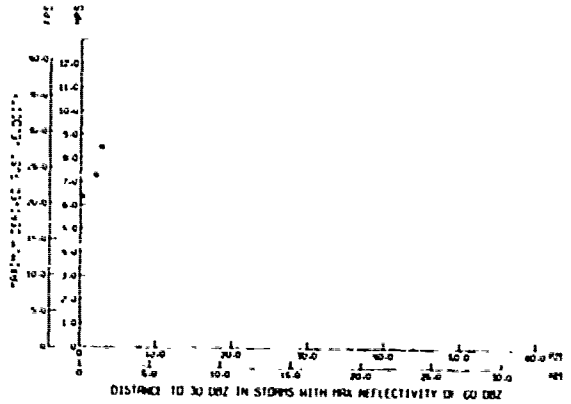

Figure 19. Distribution of derived gust velocity occurrences exceeding 6 m s^{-1} with respect to distance between occurrence and nearest portion of the 30 dBZ contour when the storm's maximum reflectivity is 60 dBZ or greater.

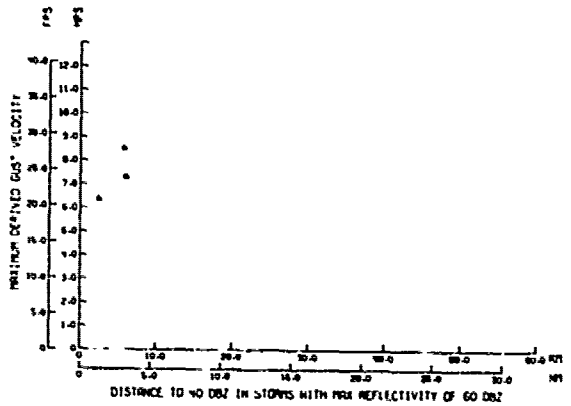

Figure 20. Distribution of derived gust velocity occurrences exceeding 6 m s^{-1} with respect to distance between occurrence and nearest portion of the 40 dBZ contour when the storm's maximum reflectivity is 60 dBZ or greater.

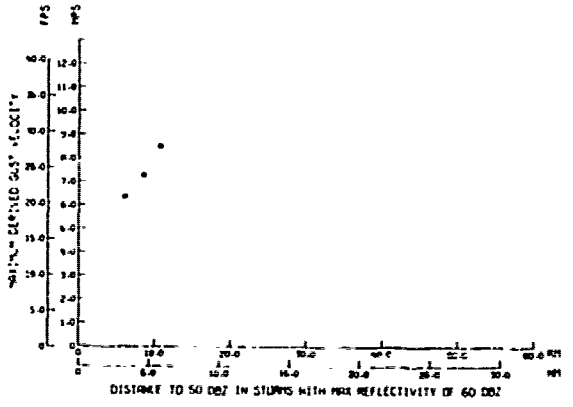

Figure 21. Distribution of derived gust velocity occurrences exceeding 6 m s-1 with respect to distance between occurrence and nearest portion of the 50 dBZ contour when the storm's maximum reflectivity is 60 dBZ or greater.

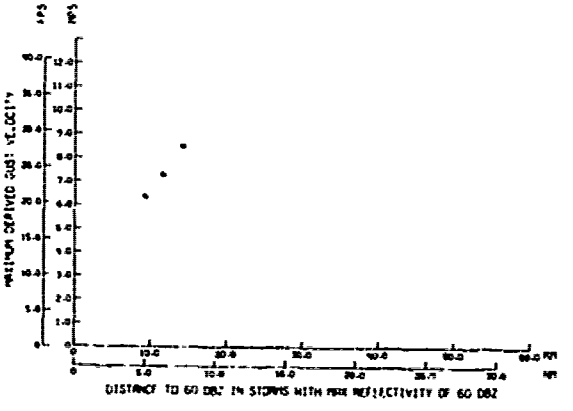

Figure 22. Distribution of derived gust velocity occurrences exceeding 6 m s-1 with respect to distance between occurrence and nearest portion of the 60 dBZ contour when the storm's maximum reflectivity is 60 dBZ or greater.

Table 3. Correlations between maxumum derived gust velocity experienced in a penetration and the maximum value of log Z_e of storm and maximum value of log Z_e along flight path.

Range of Gusts in Sample (fps)	Number in Sample	Sampled Gusts Mean (fps)	S.D. of Sampled Gusts	Mean of Max Z_e Along Track (dBZ)	S.D. of Max Z_e of Track (dBZ)	Mean Max Z_e of Storms	S.D. of Storms Max Z_e	Corr. U_{de} and Max Z_e Along Track	Corr. U_{de} and Max Z_e of Storm
0.0-44.3	108	20.73	10.13	32.5	11.4	42.6	08.6	0.380	0.394
5.0-44.3	96	23.25	7.92	33.3	11.2	43.7	06.5	0.345	0.289
10.0-44.3	96	23.25	7.92	33.3	11.2	43.7	06.5	0.345	0.289
15.0-44.3	83	24.87	7.27	35.4	09.0	44.1	06.5	0.188	0.254
20.0-44.3	57	28.10	6.52	36.8	08.4	44.6	05.9	0.046	0.290
25.0-44.3	35	32.17	5.01	38.0	08.1	46.3	05.1	-0.214	0.001
30.0-44.3	20	35.59	3.70	37.3	06.8	45.5	04.6	-0.248	0.219
35.0-44.3	11	38.22	2.35	37.3	06.5	46.8	04.6	-0.283	-0.165

Figure 23 represents a different data presentation form and shows that if severe turbulence was encountered, the maximum storm reflectivity was 40 dBZ or larger. This is in agreement with the mid-1960 studies.

7.0 Summary

A total of 153 thunderstorm penetrations having complete radar and aircraft data records, were made in the period 1973-1977. These data show characteristics similar to those produced by the mid-1960's Rough Rider Program. The correlation between turbulence and radar reflectivity along the flight path is small. The same lack of correlation is apparent in the relationship of turbulence to distance from the storm's centroid. There is a poor correlation between turbulence and distance from any specific reflectivity. Thus, this again emphasizes that with current radar and display techniques, it is the storm intensity (i.e., maximum radar reflectivity) that is most indicative of turbulence which might be expected some place in the storm system. Doppler radar appears to offer the highest potential for further defining these turbulent zones (Lee, 1977) as turbulence is due to kinematic features that can best be measured remotely with a Doppler radar.

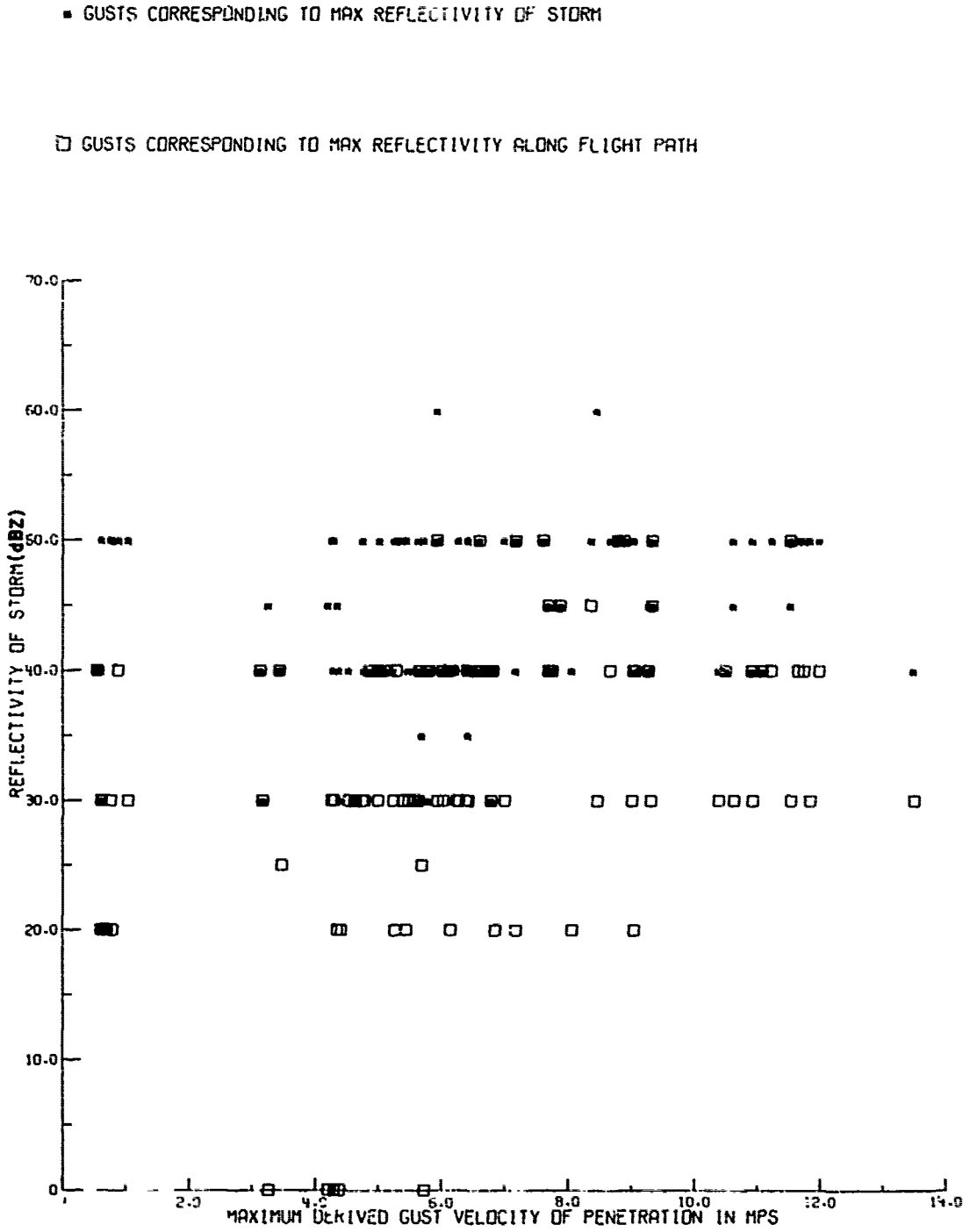

Figure 23. Distribution of maximum derived gust velocity encountered during a penetration relative to maximum radar reflectivity of storm (asterisk symbol) and maximum reflectivity along the flight path (square symbol). Solid line indicates limit line for maximum turbulence for each maximum storm reflectivity.

REFERENCES

Burnham, J. A. M., and J. T. Lee, 1969: Thunderstorm turbulence and its relationship to weather radar echoes. J. of Aircraft, Vol. 6, No. 5, 438-445.

Lee, J. T., 1965: Thunderstorm turbulence and radar echoes 1964 data studies. Proceedings, 5th Annual National Conf. on Environmental Effects on Aircraft and Propulsion Systems, NATTS Report, Princeton, N.J., 19.

Lee, J. T., 1977: Application of Doppler weather radar to turbulence measurements which affect aircraft. FAA Report No. FAA-RD-77-145.

Pratt, K. G., and W. G. Walker, 1954: A revised gust-load formula and a re-evaluation of V-G data taken on civil transport airplanes from 1933 to 1950. National Advosory Comittee for Aeronautics, Report 1206, 1-4.